

First palaeoneurological study of a sauropod dinosaur from France and its phylogenetic significance

Fabien Knoll^{1,2}, Stephan Lautenschlager³, Xavier Valentin⁴, Verónica Díez Díaz^{5,6}, Xabier Pereda Suberbiola⁷ and Géraldine Garcia⁴

¹ ARAID-Fundación Conjunto Paleontológico de Teruel-Dinópolis, Teruel, Spain

² Departamento de Paleobiología, Museo Nacional de Ciencias Naturales-CSIC, Madrid, Spain

³ School of Geography, Earth and Environmental Sciences, University of Birmingham, Birmingham, UK

⁴ Laboratoire de Paléontologie, Evolution, Paléocécosystèmes et Paléoprimatologie, Université de Poitiers, Poitiers, France

⁵ Museum für Naturkunde, Leibniz-Institut für Evolutions-und Biodiversitätsforschung, Berlin, Germany

⁶ Humboldt Universität zu Berlin, Berlin, Germany

⁷ Departamento de Estratigrafía y Paleontología, Universidad del País Vasco/Euskal Herriko Unibertsitatea, Bilbao, Spain

ABSTRACT

Despite continuous improvements, our knowledge of the palaeoneurology of sauropod dinosaurs is still deficient. This holds true even for Titanosauria, which is a particularly speciose clade of sauropods with representatives known from numerous Cretaceous sites in many countries on all continents. The data currently available regarding the palaeoneurology of titanosaurs is strongly biased towards Gondwanan forms (Argentina above all, but also India, Malawi and Australia). In contrast, the palaeoneurology of Laurasian titanosaurs is known only from a few taxa from Spain and Uzbekistan, despite the discovery in other countries of Laurasia of a number of neurocranial remains that would lend themselves well to investigations of this kind. To fill in this gap in our knowledge, we subjected a titanosaurian braincase from the uppermost Upper Cretaceous of southern France to X-ray computed tomographic scanning, allowing the generation of 3D renderings of the endocranial cavity enclosing the brain, cranial nerves and blood vessels, as well as the labyrinth of the inner ear. These reconstructions are used to clarify the phylogenetic position of the specimen from the Fox-Amphoux-Métisson site. A combination of characters, including the presence of two hypoglossal rami on the endocast, the average degree of development of the dorsal-head/caudal-middle-cerebral vein system and the relatively short and subequal lengths of the ipsilateral semicircular canals of the labyrinth, are particularly revealing in this respect. They suggest that, compared with the few other Laurasian titanosaurs for which in-depth palaeoneurological data are available, the French taxon is more derived than the distinctly more ancient, possibly non-lithostrotian titanosaur from the Uzbek site of Dzharakuduk but more basal than derived saltasaurids, such as the coeval or slightly more recent forms from the Spanish locality of Lo Hueco.

Submitted 11 April 2019

Accepted 4 October 2019

Published 18 November 2019

Corresponding author

Fabien Knoll,
knoll@fundaciondinopolis.org

Academic editor

Andrew Farke

Additional Information and
Declarations can be found on
page 17

DOI [10.7717/peerj.7991](https://doi.org/10.7717/peerj.7991)

© Copyright
2019 Knoll et al.

Distributed under
Creative Commons CC-BY 4.0

OPEN ACCESS

Subjects Evolutionary Studies, Neuroscience, Paleontology, Taxonomy

Keywords Titanosauria, Palaeoneurology, Cretaceous, Phylogeny, France

INTRODUCTION

The first observations on the palaeoneurology of sauropod dinosaurs were made almost 140 years ago (*Marsh, 1880*: unnumb. fig.). Nevertheless, the group has since been the focus of relatively scanty investigations on a few species (see in particular *Witmer et al., 2008*, and references therein; *Paulina Carabajal, Coria & Chiappe, 2008*; *Knoll & Schwarz-Wings, 2009*; *Wilson et al., 2009*; *Balanoff, Bever & Ikejiri, 2010*; *Knoll et al., 2012, 2013, 2015*; *Paulina Carabajal, 2012*; *Paulina Carabajal, Carballido & Currie, 2014*; *Sues et al., 2015*; *Martínez et al., 2016*; *Paulina Carabajal, Canale & Haluza, 2016*; *Bronzati, Benson & Rauhut, 2018*; *Paulina Carabajal et al., 2018*). This is, in part, due to the fact that braincases of sauropods are extremely rare. Sauropods are especially interesting to the palaeoneurologist because of their *Bauplan*, which features, at the extremity of a variously elongated neck, a head of conspicuously small size relative to the generally imposing body (*Sander et al., 2011*; *Hallett & Wedel, 2016*). The size of the body reaches the maximum known in any land tetrapod within a speciose clade of Cretaceous sauropods, the Titanosauria (see e.g., *Benson et al., 2014*). Over the last decade, our knowledge of the palaeoneurology of titanosaurian sauropods has dramatically improved. While the endocranial morphology of titanosaurs has long been known only in *Jainosaurus septentrionalis* (*Huene & Matley, 1933*) from the Maastrichtian of India, a considerable amount of new data on the endocranial and inner ear morphology in taxa from Argentina, Spain, India, Uzbekistan, Australia and Malawi have recently been gathered (*Paulina Carabajal, 2012*; *Knoll et al., 2013, 2015*; *Paulina Carabajal, Filippi & Knoll, 2015*; *Sues et al., 2015*; *Martínez et al., 2016*; *Poropat et al., 2016*; *Andrzejewski et al., 2019*). However, this represents only a diminutive fraction of titanosaurian taxic diversity. In fact, while the descriptions of new titanosaur species are regularly published, they rarely include any neurocranial remains (*Wilson et al., 2016*; for recently described titanosaurs lacking braincase material see e.g., *Calvo & Gonzalez Riga, 2019*; *Gorscak & O'Connor, 2019*). Nevertheless, a number of titanosaurian braincases have yet to be examined from a palaeoneurological viewpoint (through modern imaging technologies or otherwise). This holds especially true for the Upper Cretaceous of Europe. European specimens represent significant data to help assess the diversity of titanosaurs that are being neglected. The aim of the present article is to describe the digital endocast of an isolated braincase of an unnamed titanosaur from the Upper Cretaceous of the Provence-Alpes-Côte d'Azur region of southern France and to build on this reconstruction to clarify the phylogenetic position of the specimen.

MATERIALS AND METHODS

The present study focuses on a reconstruction of the endocranial and labyrinthine cavities of a previously described, but undiagnosed braincase, FAM 03.064, from the Campanian locality of Fox-Amphoux-Métisson (Montmeyan syncline), Var, southeastern France (*Díez Díaz et al., 2012*). The specimen comes from the “Grès à Reptiles” Formation and more specifically

from a sandstone deposit yielding wood, invertebrates and a variety of vertebrates (selachians, bony fishes, turtles, squamates, crocodylians and dinosaurs). The dinosaur fauna itself is diverse (theropods, sauropods, ankylosaurs and ornithopods), although only sauropod dental and cranial specimens have been examined in detail so far ([Díez Díaz et al., 2012](#)).

It was identified as belonging to Titanosauria on the basis of a combination of characters purportedly not found outside this clade (including a pair of well-defined crescentic transverse nuchal crests on the parietal and other features involving different neurocranial bones; see [Díez Díaz et al., 2012](#): p. 635). Its precise affinities with other titanosaurs could not be clarified, except for the fact that several aspects of its morphology set it apart from other European titanosaurian braincases ([Díez Díaz et al., 2012](#): p. 635), all of which either Campanian or Maastrichtian in age.

To produce a three-dimensional reconstruction of the endocast of the cranial cavity and endosseous labyrinth of the inner ear, the specimen was subjected to computed tomographic (CT) scanning at the Université de Poitiers (Poitiers, France), using a EasyTom XL duo (RX-Solutions, Chavanod, France) with a voltage of 130 kV and a current of 440 μ A. The dataset consisted of 1165 slices ($1089 \times 1034 \times 1165$ pixels, 0.116 mm voxel size) in tiff format.

The CT data were imported into Avizo 7.0 (Visualisation Science Group, Burlington, MA, USA) for image segmentation and digital reconstruction. Anatomical structures of interest (endocasts, endosseous labyrinths, neurovascular structures) were labelled using Avizo's segmentation editor. The magic wand tool was used where possible to perform the segmentation semi-automatically (with thresholds for bone set to a greyscale value larger than 35,000, a value of 25,000–35,000 for sediment infill and values below 5,000 for air-filled cavities). In regions with poor contrast between matrix, bone and structures of interest the paintbrush tool was used for manual segmentation. 3D surface models and volumes were created to visualize the segmented structures and to illustrate this article with traditional figures ([Figs. 1–3](#)). In addition, surface models of the individual structures were downsampled to a degree that allowed for small file sizes, but preserved all details, and were exported as separate OBJ files for the creation of the interactive 3D model of [Fig. S1](#), as outlined in [Lautenschlager \(2014: pp. 116-117\)](#) using Adobe 3D reviewer (Adobe Systems Inc., San Jose, CA, USA).

The palaeoneurology of FAM 03.064 is compared below with that of the other titanosaurs from the Late Cretaceous of Eurasia and India for which endocasts (be they physical or digital) of the cranial cavity and endosseous labyrinth have been described ([Table 1](#)) as well as with species from different times and locations when appropriate.

RESULTS

Systematic palaeontology

Dinosauria [Owen, 1842](#)

Saurischia [Seeley, 1888](#)

Sauropoda [Marsh, 1878](#)

Titanosauria [Bonaparte et Coria, 1993](#)

Titanosauria indet.

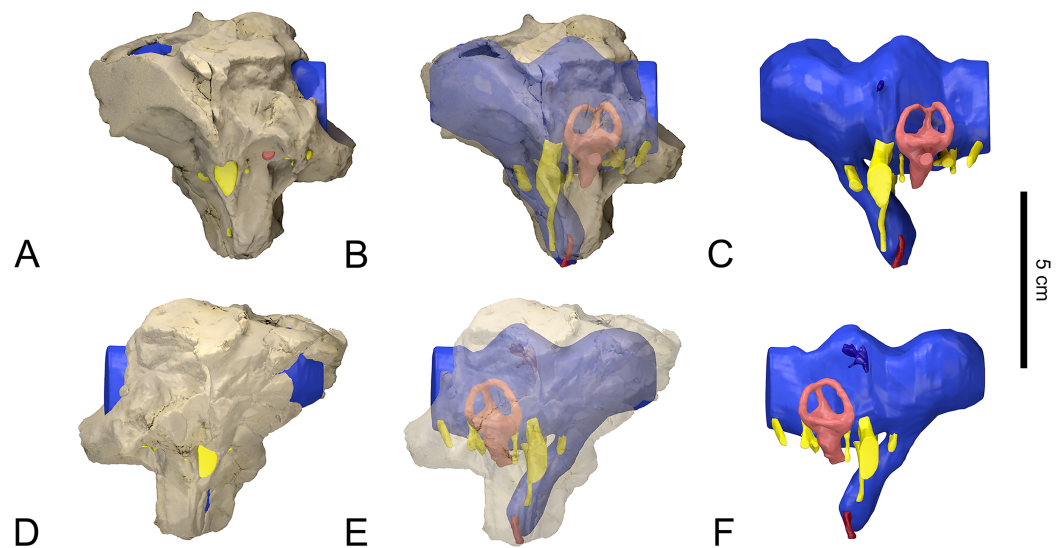


Figure 1 Surface-rendered CT-based reconstructions of the braincase, cranial endocast and associated soft tissue structures of the indeterminate titanosaur specimen (FAM 03.064) from the Late Cretaceous of Fox-Amphoux-Métisison, France. Bone rendered opaque (A, D), made semi-transparent (B, E) and removed (C, F). In left (A–C) and right (D–F) lateral views.

Full-size [DOI: 10.7717/peerj.7991/fig-1](https://doi.org/10.7717/peerj.7991/fig-1)

Description and comparison

As the median part of the conjoined frontals has broken away in FAM 03.064, the top of the cerebrocast had to be inferred to a degree. The same holds true for the ventral side of the endocast due to the incomplete state of preservation of the orbitosphenoids (the left rostralateral region of the cerebrocast is mirrored from the right side, which could be reconstructed). Apart from these minor aspects, the CT scan data permitted a comprehensive rendering of the cranial endocast and endosseous labyrinths (Figs. 1–3). Most cranial nerves, as well as major vascular structures, could be reconstructed on both sides. Reconstructions of both the right and left labyrinths could also be achieved.

Brain endocast

The incompleteness of FAM 03.064 rostradorsally makes it impossible to gauge the length of the olfactory tract (Fig. 1). In this regard, the specimen is similar to others. For example, the state of GSI K27/497 prevents making appropriate observations regarding the olfactory tracts and bulbs in *J. septentrionalis* (Wilson *et al.*, 2009: fig. 7). The condition of CCMGE 628/12457 is worse still, as both frontals seem to be missing entirely in this specimen of indeterminate titanosaur (Sues *et al.*, 2015: figs 2C; Witmer, 2019). In contrast, the frontals of MPCM-HUE-8741, a specimen that is here tentatively attributed to *Lohuecotitan pandafilandi*, are well preserved. They cover very short olfactory tracts rostrally (Knoll *et al.*, 2013: figs 3A, C, D, S1, S2, S3). In MPCM-HUE-1667, an unnamed lithostrotian titanosaur, the olfactory tracts could be reconstructed in their entirety. They are extremely short (Knoll *et al.*, 2015: figs 4, 5C, D, S1). This is consistent with shortened nasal bones and, therefore, external nares with greatly retracted caudal

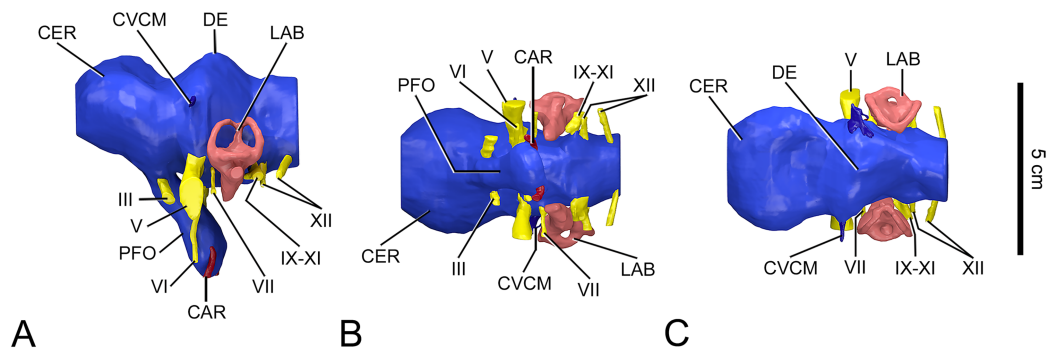


Figure 2 Surface-rendered CT-based reconstructions of the cranial endocast and associated soft tissues structures of the indeterminate titanosaurian braincase (FAM 03.064) from the Late Cretaceous of Fox-Amphoux-Métisson, France. In lateral (A), ventral (B) and dorsal (C) views. Abbreviations: III, oculomotor nerve; V, trigeminal nerve; VI, abducens nerve; VII, facial nerve; IX-XI, glossopharyngeal and vagoaccessory nerves; XII, hypoglossal nerve; CAR, internal carotid artery; CER, cerebrum; CVCM, caudal middle cerebral vein; DE, dural expansion; LAB, labyrinth; PFO, pituitary body. Full-size [DOI: 10.7717/peerj.7991/fig-2](https://doi.org/10.7717/peerj.7991/fig-2)

margin as observed in other titanosaurs (*Curry Rogers & Forster, 2004; Wilson, 2005; Martínez et al., 2016; Wilson et al., 2016*) and indeed many other sauropods.

As in other titanosaurs, especially derived forms such as MPCM-HUE-1667 (*Knoll et al., 2015: figs 4, S1*), the endocast of FAM 03.064 appears fairly straight in lateral view (*Fig. 1*). This stands in sharp contrast with the endocast of the basal titanosauriform *Giraffatitan brancai*, the flexures of which make it look more clearly sigmoid in lateral view (*Knoll & Schwarz-Wings, 2009: figs 1, 2A, B*). In fact, an endocast that appears strongly sigmoid in lateral view is the plesiomorphic condition in sauropodomorphs (see e.g., *Sereno et al., 2007: fig. 1G*). The endocast of FAM 03.064 is lageniform in outline in dorsal view (*Fig. 2C*), strongly recalling the homologous portions of the endocasts of both *L. pandafilandi* (*Knoll et al., 2013: figs 3C, S1, S2, S3*) and MPCM-HUE-1667 (*Knoll et al., 2015: fig. 5D, S1*) in that respect. The cerebrocast is marked by a caudomedian depression dorsally, which gives it a C-shaped aspect in dorsal view (*Fig. 2C*). A roughly similar configuration is seen in *L. pandafilandi* (*Knoll et al., 2013: figs 3C, S1, S2, S3*), which was interpreted as being due to paired longitudinal dural venous sinuses coursing dorsolaterally over the cerebral region (*Knoll et al., 2013: p. 7*). The cerebrocast constitutes the widest portion of the endocast. The forebrain region is separated from the midbrain-hindbrain complex by a marked constriction (*Figs. 1 and 2*), which is caused by a sturdy internal laterosphenoid pillar. A second medial narrowing affects the caudal quarter of the endocast (*Figs. 1 and 2*). It corresponds to the space occupied by the otic capsule within the lateral wall of the braincase. A tiny knob dorsal to the facial nerve on the right side of the endocast (best observable in *Fig. S1* when the right labyrinth is unticked) may be due to a diminutive fossa auriculæ cerebelli (which in life housed the cerebellar flocculus; see e.g., *Ferreira-Cardoso et al., 2017*). This is the only tangible indication of the cerebellum. No visible relief on the endocast is present in *J. septentrionalis* (*Wilson et al., 2009: fig. 7A*), *L. pandafilandi* (*Knoll et al., 2013: figs 3A, S1, S2, S3*), MPCM-HUE-1667 (*Knoll et al., 2015: figs 4, S1*) or CCMGE 628/12457 (*Sues et al., 2015: fig. 3A*).

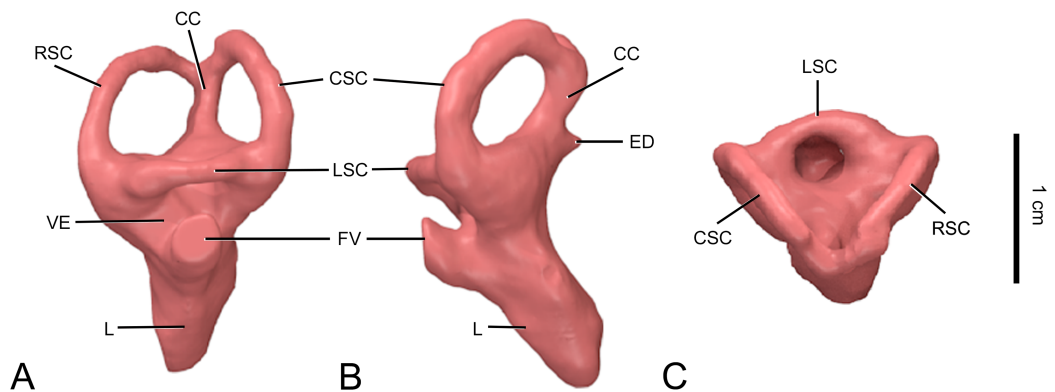


Figure 3 Surface-rendered CT-based reconstruction of the left endosseous labyrinth of the indeterminate titanosaurian braincase (FAM 03.064) from the Late Cretaceous of Fox-Amphoux-Métisson, France. In lateral (A), caudal (B) and dorsal (C) views. Abbreviations: CC, common crus; CSC, caudal semicircular canal; ED, endolymphatic duct; FV, oval window; L, lagena; LSC, lateral semicircular canal; RSC, rostral semicircular canal; VE, vestibule.

Full-size [DOI: 10.7717/peerj.7991/fig-3](https://doi.org/10.7717/peerj.7991/fig-3)

Table 1 Titanosaurian endocasts used for comparison in this study.

Specimen	Taxon	Age	Country
GSI K27/497 (Huene & Matley, 1933: fig. 6; Wilson et al., 2009: fig. 7)	<i>Jainosaurus septentrionalis</i> (Huene et Matley, 1933)	Maastrichtian	India
MPCM-HUE-8741 (Knoll et al., 2013: figs 3, 4, S1, S2, S3)	<i>Lohuecotitan pandafilandi</i> (Diez Díaz et al., 2016)	Campanian	Spain
MPCM-HUE-1667 (Knoll et al., 2015: figs 4, 5, 7, S1)	Lithostrotia indet.	Campanian	Spain
CCMGE 628/12457 (Sues et al., 2015: figs 3, 4, Witmer, 2019)	Titanosauria indet.	Turonian	Uzbekistan

In fact, embossments related to the cerebellar flocculus are rare in sauropod endocasts. They are best developed in *G. brancai* (Knoll & Schwarz-Wings, 2009: figs 1, 2A–D), in which they lodge themselves in small but sharply delimited dents on the medial surface of the prootic (Janensch, 1935–1936: fig. 116). In basalmost sauropodomorphs (see e.g., Bronzati et al., 2017: fig. 2), the floccular fossae may be more developed than in more derived forms.

Despite the poor preservation of the cranial vault in the forebrain region in FAM 03.064, it can be determined that this part of the brain was not covered by a large, irregularly-shaped dural expansion (Figs. 1, 2A and 2C). This is similar to what can be observed on the endocasts of both Lo Hueco lithostrotians (Knoll et al., 2013: figs 3A, C, S1, S2, S3, Knoll et al., 2015: figs 4, 5A, D, S1), which lack a voluminous rostral dural expansion, but this is in contrast with the situation in a number of other sauropods, such as *G. brancai* (Knoll & Schwarz-Wings, 2009: figs 1, 2A, B) and the putative basal lithostrotian *Sarmientosaurus musacchioi* (Martínez et al., 2016: figs 9A, D, S1), for instance, whose endocasts show crag-like enlargements that, presumably, are indicative of a sizeable

venous sinus. The hindbrain of FAM 03.064 appears to support a relatively large caudal dural expansion (Figs. 1, 2A and 2C), which may be due to a confluence between the transverse (“middle cerebral vein”), dorsal sagittal and occipital sinuses. A very similar configuration is found in MPCM-HUE-1667 (Knoll et al., 2015: figs 4, 5A, B, D, S1) and the endocast of *J. septentrionalis* (Wilson et al., 2009: fig. 7A) is comparable in this respect. In its plain rather than complicated shape, this caudal dural expansion differs from those in CCMGE 628/12457 (Sues et al., 2015: figs 3A, B, D, E), *S. musacchioi* (Martínez et al., 2016: figs 9A, B, D, S1), *G. brancai* (Knoll & Schwarz-Wings, 2009: figs 1, 2A, B) and a number of more basal sauropods. The caudal half of the endocast of *L. pandafilei* does not display any large caudal dural expansion, but only a minor convoluted protrusion (Knoll et al., 2013: figs 3A–C, S1, S2, S3). All in all, FAM 03.064 resembles MPCM-HUE-1667 (Knoll et al., 2015: figs 4, 5) and *J. septentrionalis* (Wilson et al., 2009: fig. 7) closely, as far as the overall morphology of the endocast is concerned.

As in most sauropodomorphs (Witmer et al., 2008), the endocast of FAM 03.064 exposes a large hypophysis (pituitary) that extends caudoventrally (Figs. 1, 2A and 2B). Similar to *G. brancai* (Knoll & Schwarz-Wings, 2009: figs 1, 2A, B) but in contrast with most other sauropods (see e.g., Witmer et al., 2008: figs 6.8, 6.9; Balanoff, Bever & Ikejiri, 2010: fig. 10), the infundibulum is not constricted (Fig. 1). The hypophysis is claviform in rostral or caudal view but rather musiform (with the concavity situated rostrally) in lateral view (Fig. 1). It is the widest at the level of the entrance of the internal carotid arteries. The long axis of the hypophysis makes an angle of about 65° with that of the lateral semicircular canal (Fig. 1). This is more obtuse than in *L. pandafilei* (~55°; Knoll et al., 2013: figs 3A, S1, S2, S3), MPCM-HUE-1667 (~45°; Knoll et al., 2015: figs 4, S1) and also, although to a lesser degree, CCMGE 628/12457 and *Malawisaurus dixeyi* (~60°; Sues et al., 2015: fig. 3A; Andrzejewski et al., 2019: figs 2A, S1). This angle is also about 65° in the *Lithostrotia incertae sedis Bonatitan reigi* (Paulina Carabajal, 2012: fig. 2A), not far off the 70° observed in *G. brancai* (Knoll & Schwarz-Wings, 2009: figs 1, 2A, B). The morphology of the hypophysis in the endocast of FAM 03.064 is very different from that in CCMGE 628/12457 (Sues et al., 2015: fig. 3A, B, C, E), which is composed of a slender but humpbacked proximal half and a bulbous distal half. In contrast, it compares well with the hypophysis of MPCM-HUE-1667 (Knoll et al., 2015: figs 4, 5A, B, C, S1). However, in the latter the caudoventral orientation of the hypophyseal body is attained through a bend of the infundibular stalk (as in *L. pandafilei*; Knoll et al., 2013: figs 3A, S1, S2, S3), whereas in FAM 03.064 the infundibulum is in line with the rest of the hypophysis (Fig. 1; like in CCMGE 628/12457; Sues et al., 2015: fig. 3A).

Cranial nerves

Neither orbitosphenoid is complete enough in FAM 03.064 to allow reconstructing the optic nerve (CN II).

The oculomotor nerve (CN III) emerges from the endocast in the lateral surface of the infundibulum (Figs. 2A and 2B). It then courses ventrolaterally to leave the braincase through the suture between the orbitosphenoid (rostrally) and the laterosphenoid (caudally), that is in the orbit. The oculomotor nerve is inadequately known in

J. septentrionalis (Wilson et al., 2009), but there does not appear to be any meaningful differences in this respect between FAM 03.064 and *L. pandafileandi* (Knoll et al., 2013: figs 3A, D, S1, S2, S3), MPCM-HUE-1667 (Knoll et al., 2015: figs 4, 5A, C, S1) and CCMGE 628/12457 (Sues et al., 2015: figs 3A, C, E, Witmer, 2019).

The trochlear nerve (CN IV) could not be reconstructed in FAM 03.064. It is possibly represented on the lateral wall of the braincase by only a tiny foramen on the rostral margin of the laterosphenoid (Díez Díaz et al., 2012: fig. 5B, E, F), but the resolution of the CT data allowed no unambiguous reconstruction of the nerve canal. If it could have been traced digitally, it may have looked fairly similar in diameter and location to the trochlear nerve in MPCM-HUE-1667 (Knoll et al., 2015: figs 3D, S1).

The trigeminal nerve (CN V) is, as expected, the biggest of the cranial nerves (Fig. 2). Its largest diameter is much greater than that of the metotic group (CN IX-XI; vide infra). In cross section, the trigeminal nerve forms an ellipse with a dorsoventrally oriented major axis all along its ventrolateral course from the endocast to the external foramen on the laterosphenoid-prootic suture. So, the in vivo division of this nerve into rostral (ophthalmic, CN V₁) and caudal (maxillomandibular, CN V_{2,3}) rami is not patent osteologically (even though the trigeminal foramen does have a somewhat cordiform rim laterally). The configurations of the trigeminal nerve in FAM 03.064 and MPCM-HUE-1667 (Knoll et al., 2015: figs 4, 5A, C, D, S1) are similar and no relevant difference with CCMGE 628/12457 (Sues et al., 2015: figs 3A, C, E; Witmer, 2019) can be detected in this regard. In *L. pandafileandi* (Knoll et al., 2013: figs 3, S1, S2, S3), the intraosseous path of the trigeminal nerve appears shorter as it is directed more laterally. Little is known about the trigeminal nerve in *J. septentrionalis* (Wilson et al., 2009).

The abducens nerve (CN VI) emerges ventrally from the pontine portion of the brainstem, ventral to the trigeminal nerve (Figs. 2A and 2B). It then courses rostroventrally, gets past the pituitary body laterally, very closely (a solid but thin wall of bone separates them), and leaves the braincase from the rostral surface of the parabasisphenoid (Fig. 1; see also Díez Díaz et al., 2012: figs 3A, 4B, C). As far as the state of preservation permits to determine, the configuration was similar in *L. pandafileandi* (Knoll et al., 2013: figs 3B, D, S1, S2, S3). The abducens nerves either penetrate the pituitary fossa (MB.R.2180.22.1-4, M.B.R.2384) or pass in its periphery (MB.R.2223.1) in *G. brancai* (Janensch, 1935–1936: p. 259, figs 117, 118, pl. 13 fig. 1a; Knoll & Schwarz-Wings, 2009: figs 1, 2A, B; F Knoll, 2009, personal observations). In *Europasaurus holgeri*, another basal titanosauriform, the abducens nerves pierce the floor of the endocranial cavity close to one another, but then diverge so that they do not enter the pituitary fossa (A Schmitt, F Knoll & E Tschopp, 2015, personal observations). In most sauropods, the abducens canal cohere with the pituitary fossa (see e.g., Witmer et al., 2008; Knoll et al., 2012; Paulina Carabajal, Carballido & Currie, 2014). Whereas the abducens nerve flanks the hypophysis closely in FAM 03.064, it passes at bay in MPCM-HUE-1667 (Knoll et al., 2015: figs 5A, B, C, S1).

The facial nerve (CN VII) emerges from the brainstem about halfway between the trigeminal nerve (CN V) and the inner ear region (Figs. 2A and 2B), close to the vestibulocochlear nerve (CN VIII). It orientates ventrolaterally in parallel with the trigeminal nerve. After running within the prootic, the facial nerve leaves the braincase

on the caudal side of the prootic crest. Externally, a main branch of it diverges to run ventrally on the prootic and then on the parabasisphenoid lateral surface, as a well-defined, fairly straight channel in the rostroventral sector of the middle ear recess demonstrates (see [Díez Díaz et al., 2012](#): figs 4, 5E, F). The intraosseous route of the facial nerve is similar in FAM 03.064, MPCM-HUE-1667 ([Knoll et al., 2015](#): figs 5A, C, S1) and CCMGE 628/12457 ([Sues et al., 2015](#): figs 3A, C; [Witmer, 2019](#)). Unfortunately, the course of the facial nerve is not well known in *L. pandafilei* ([Knoll et al., 2013](#): figs 3D, S1, S2, S3), nor is it in *J. septentrionalis* ([Wilson et al., 2009](#): fig. 7A). No channel for the facial nerve is present on the external surface of the braincases of either *L. pandafilei* ([Knoll et al., 2013](#): figs S1, S2, S3), CCMGE 628/12457 ([Sues et al., 2015](#): figs 1A, C, 2A; [Witmer, 2019](#)) or, as it seems, *J. septentrionalis* (GSI K27/497; [Wilson et al., 2009](#): fig. 4A). In contrast, a channel, functionally equivalent but not so distinct structurally, is present on MPCM-HUE-1667 ([Knoll et al., 2015](#): figs 3C, S1).

Whereas the cochlear branch of the vestibulocochlear nerve (CN VIII) could not be traced in the FAM 03.064 CT scan data, the vestibular one could be visualized as it innervates the vestibular labyrinth in the region of the ampulla of the rostral semicircular canal ([Fig. S1](#)). No part of the vestibulocochlear nerve could be reconstructed in *L. pandafilei* ([Knoll et al., 2013](#)), and no information is available either in this respect in *J. septentrionalis* ([Wilson et al., 2009](#)). In contrast, this zone could be segmented to the same limited extent as in FAM 03.064 in MPCM-HUE-1667 ([Knoll et al., 2015](#): fig. S1). The configuration is similar in these two specimens, with a short vestibular branch of the vestibulocochlear nerve connected with the ampulla of the rostral semicircular canal. Connections of the inner ear with the endocranial space have been rendered in exceptional quality in CCMGE 628/12457 ([Sues et al., 2015](#); [Witmer, 2019](#)). Thus, CCMGE 628/12457 shows an additional division of the vestibular branch of the vestibulocochlear nerve compared with FAM 03.064 (as well as the endolymphatic duct). This supplementary division of the vestibular branch could be segmented also in *S. musacchioi* ([Martínez et al., 2016](#): fig. S1), in which it is spatially closer to that innervating the ampulla of the rostral semicircular canal than in CCMGE 628/12457.

The glossopharyngeal and vagoaccessory nerves (CN IX-XI) are combined together and with other structures into a metotic group situated between the labyrinth of the inner ear rostrally and the rostral hypoglossal branch caudally ([Figs. 2A and 2B](#)). The metotic group extends ventrolaterally, filling out the caudal part of the metotic cavity (cavum metoticum), which is cordiform in outline in ventrolateral view of the braincase. This caudal lobe of the metotic cavity accommodates the metotic foramen, whereas the rostral lobe, of smaller size, houses the oval window. As far as preservation allows the observation of this region, the configuration seems to have been similar in *L. pandafilei* ([Knoll et al., 2013](#): figs S1, S2, S3). In contrast, the metotic foramen and oval window are not confined into a hollow of heart-shaped contour in MPCM-HUE-1667 ([Knoll et al., 2015](#): fig. S1) or CCMGE 628/12457 ([Sues et al., 2015](#); [Witmer, 2019](#)). In these specimens, these openings lie at the bottom of the shapeless, wider depression limited by the prootic crest rostrally and the tuberal crest caudally. The condition is comparable in *S. musacchioi* ([Martínez et al., 2016](#): fig. S1) and *G. brancai* (MB.R.2180.22.1-4; [F Knoll, 2009](#),

personal observations), suggesting that the conformation of the middle ear (tympanic) recess in FAM 03.064 and *L. pandafilei* (recessed metotic cavity) is derived.

We previously associated a bilateral foramen at the base of the occipital condyle to the hypoglossal (XII) nerve (Díez Díaz *et al.*, 2012: fig. 5C–F). CT scan data confirm this, but also reveal the presence of another hypoglossal (XII) canal about 8 mm more rostrally, which opens onto the caudal wall of the middle ear recess (Figs. 1 and 2). This rostral branch of the hypoglossal has a lesser diameter and extends in a more ventral direction than the caudal one. Only a caudal (i.e., one that shows up externally in a caudal situation with respect to the tuberal crest) hypoglossal branch was identified in *L. pandafilei* (Knoll *et al.*, 2013: figs 3A, D, S1, S2, S3), MPCM-HUE-1667 (Knoll *et al.*, 2015: figs 4, 5C, D, S1) and *J. septentrionalis* (Wilson *et al.*, 2009: fig. 7). However, a configuration similar to FAM 03.064 is observed in CCMGE 628/12457 (Sues *et al.*, 2015: fig. 3A, C). This does not indicate close affinities between FAM 03.064 and CCMGE 628/12457 (see Discussion below) as the same configuration is also described in *G. brancai* (Janensch, 1935–1936: p. 260).

Endocranial vasculature

Only two vascular structures could be reconstructed digitally in FAM 03.064. Díez Díaz *et al.* (2012) recognized one little foramen in the orbital region as the outlet of an orbitocerebral vein, but this could not be traced digitally. A similar structure was identified in MPCM-HUE-1667, but was not reconstructed either (Knoll *et al.*, 2015: p. 17). Although none is apparent on the endocast of *J. septentrionalis* (Wilson *et al.*, 2009: fig. 7), it is not possible to say if a similar slender cerebral vasculature was present and the rostralateral braincase region is poorly preserved in *L. pandafilei* (Knoll *et al.*, 2013: figs 1B, 2B, S1, S2, S3) and CCMGE 628/12457 (Sues *et al.*, 2015: figs 2A, B, C; Witmer, 2019). The only venous structure that could be reconstructed in FAM 03.064 is a vein that emerges from a sinus that is dorsal to the trigeminal nerve in the dorsoventral axis, and leaves the endocranial cavity via the occipital plate (Figs. 1, 2A and 2C). This is part of the dorsal-head/caudal-middle-cerebral vein system, which is unnoticeable in *L. pandafilei* (Knoll *et al.*, 2013: figs 3A, B, C, S1, S2, S3), MPCM-HUE-1667 (Knoll *et al.*, 2015: figs 4, 5A, B, D, S1) and *J. septentrionalis* (Wilson *et al.*, 2009: fig. 7A). A caudal middle cerebral vein is present in CCMGE 628/12457 (Sues *et al.*, 2015: figs 3A, B, D; Witmer, 2019), but it is different from that in FAM 03.064, notably because it orientates caudolaterally from the outset instead of extending laterally. In contrast, an approximately similarly orientated caudal middle cerebral vein is present in *B. reigi* (Paulina Carabajal, 2012: figs 1–3).

The cerebral carotid arteries are the main vascular structures that could be traced (Figs. 1, 2A and 2B). The two contralateral vessels are farther apart in FAM 03.064 and CCMGE 628/12457 (Sues *et al.*, 2015; Witmer, 2019) than in MPCM-HUE-1667 (Knoll *et al.*, 2015: fig. S1). In FAM 03.064 and MPCM-HUE-1667 (Knoll *et al.*, 2015: fig. S1), they diverge by about 40° when seen in caudal view of the endocasts, and by about 70° in CCMGE 628/12457 (Sues *et al.*, 2015; Witmer, 2019). A basilar artery is supposed to have originated from the caudal ramus of the carotid and run caudalward on the ventral

surface of the brainstem. In FAM 03.064, no evidence of the basilar artery is detectable on the endocast, neither as a canal through the dorsum sellae between the pituitary and the hindbrain, as in CCMGE 628/12457 (Sues *et al.*, 2015; Witmer, 2019) and *B. reigi* (Paulina Carabajal, 2012: fig. 3), for examples within Titanosauria, nor as a groove on the floor of the caudal portion of the braincase, as in the diplodocoid *Dicraeosaurus hansemanni* (MB.R.2378.1-5; F Knoll, 2009, personal observations). In FAM 03.064, the basal artery might have left the endocranial cavity to run on the ventral side of the neck of the occipital condyle in the groove noted by Díez Díaz *et al.* (2012: fig. 5C, F).

Inner ear

Both endosseous labyrinths could be reconstructed in FAM 03.064 (Figs. 2 and 3). They are arched medially, mimicking as they do the curvature of the internal surface of the braincase cavity at this place (i.e., the space constraints in this region of the braincase shape both the labyrinths and the portion of the main endocranial cavity between the two otic capsules).

The rostral and caudal semicircular canals are subequal in length (Fig. S1; Table 2). Indeed, the caudal semicircular canal of the left labyrinth appears to be slightly taller than the rostral semicircular canal, but the situation is reverse on the right side, implying suboptimal sensitivity or, in other words, relaxed selective constraints on gaze stabilization and other vestibular-controlled functions. Both vertical semicircular canals are significantly longer than the lateral semicircular canal (Fig. 3; Table 2). Titanosaurs were considered as being characterized by vertical semicircular canals of subequal lengths (Paulina Carabajal, 2012; Knoll *et al.*, 2015). Indeed, CCMGE 628/12457, *L. pandafilei*, MPCM-HUE-1667 and *J. septentrionalis* (ISI R162) have all relatively contracted vestibular regions (see Knoll *et al.*, 2015: fig. 6). However, a more basal form, such as *S. musacchioi* (Martínez *et al.*, 2016: figs 11, S1), shows a rostral semicircular canal that is intermediate in development between that of *G. brancai* (Knoll *et al.*, 2012: fig. 6) and those of these more advanced lithostrotian titanosaurs (Fig. 4). The two vertical semicircular canals diverge at about 70° (Fig. 3C), which falls between the configurations observed in *L. pandafilei* (Knoll *et al.*, 2013: figs S1, S2, S3) and MPCM-HUE-1667 (Knoll *et al.*, 2015: figs 7C, S1). The divergence angle of the two vertical semicircular canals is wider in both CCMGE 628/12457 (Sues *et al.*, 2015: fig. 4B; Witmer, 2019) and *J. septentrionalis* (ISI R162; Sues *et al.*, 2015: fig. 4E).

The lagena is relatively short in FAM 03.064 (Figs. 3A and 3B; Table 2). The relative length of the lagena varies within advanced lithostrotians, such as CCMGE 628/12457 (Sues *et al.*, 2015: fig. 4A, C; Witmer, 2019), *L. pandafilei* (Knoll *et al.*, 2013: figs 4, S1, S2, S3), MPCM-HUE-1667 (Knoll *et al.*, 2015: figs 7A, B, S1) and *J. septentrionalis* (ISI R162; Sues *et al.*, 2015: fig. 4D, F). Nonetheless, it is shorter than in more primitive forms such as *S. musacchioi* (Martínez *et al.*, 2016: figs 11A, B, S1).

DISCUSSION

Considerable advances in our understanding of titanosaurian endocranial anatomy over the last few years have been paralleled by substantial progress in our perception of the

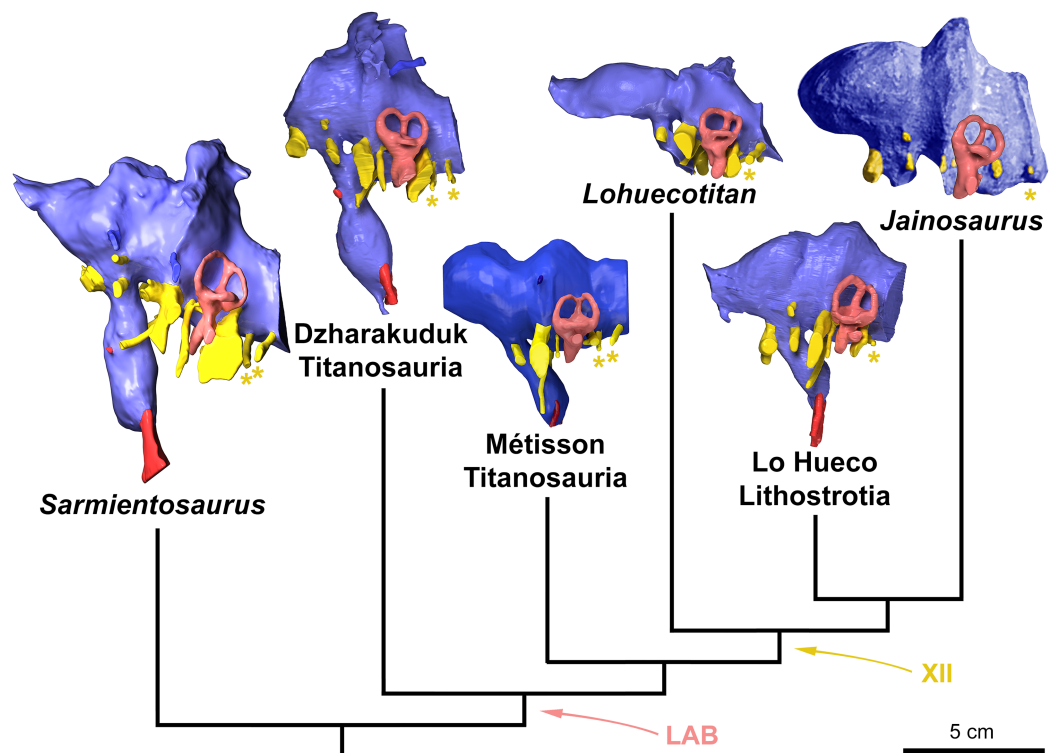


Figure 4 Endocasts of the most relevant sauropod taxa discussed in the text in a phylogenetic context. From left: *Sarmientosaurus musacchioi* (MDT-PV 2, from [Martínez et al., 2016](#)), indeterminate titanosaur from Uzbekistan (CCMGE 628/12457, from [Sues et al., 2015](#)), *Lohuecotitan pandafilandi* from Spain (MPCM-HUE-8741, right side mirrored, from [Knoll et al., 2013](#)), indeterminate titanosaur from Spain (MPCM-HUE-1667, from [Knoll et al., 2015](#)) and *Jainosaurus septentrionalis* (composite). In left lateral view. All are digital endocasts, save for *Jainosaurus septentrionalis*, which is a montage of a photograph of the physical endocast made from the lectotypic braincase (GSI K27/497, right side mirrored and colored, from [Wilson et al., 2009](#)) combined with the digital reconstruction of the endosseous labyrinth from a different specimen referred to the same species (ISI R162, from [Knoll et al., 2012](#)). LAB and XII indicate synapomorphic reduction of the labyrinth of the inner ear (pink) and loss of one hypoglossal canal (asterisks) in the neurocranial wall, respectively. Note the trend towards a reduction of the dural membrane and associated venous channels, resulting in the uncluttered endocasts of most advanced titanosaurs. [Full-size](#) DOI: 10.7717/peerj.7991/fig-4

topology of titanosaurian phylogeny (see in particular [Sallam et al., 2018](#); [Gorscak & O'Connor, 2019](#); [Mannion et al., 2019a, 2019b](#)), which had been particularly labile until then. As it turned out, the study of the osteology of FAM 03.064 through external observation did not provide insight regarding the phylogenetic position of the species to which it belongs within Titanosauria ([Díez Díaz et al., 2012](#)). Nevertheless, palaeoneurological information uncovered in the present work and evaluated in the light of recent thorough phylogenetic analyses of Titanosauria permits some clarification to be provided on this issue ([Fig. 4](#)). Naturally, not all palaeoneurological features are equally valuable indicators of phylogenetic relationships. For example, it seems that the lateral distance with which the abducens nerve makes its way past the pituitary is particularly prone to homoplasy. Indeed, in a variety of titanosaurs, such as MPCM-HUE-1667 ([Knoll et al., 2015](#): figs 5A, B, C, S1), which is most likely more derived than FAM 03.064,

Table 2 Measurements of the endocast of the indeterminate titanosaurian braincase (FAM 03.064) from the Late Cretaceous of Fox-Amphoux-Métisson, France, and some of its components.

Component	Length (cm)	Width (cm)	Diameter (cm)	Volume (cm ³)
Endocast	6.44	4.49	–	52
Cerebral hemispheres	2.58	3.68	–	21
Lagena (average)	1.00	0.62	–	0.3
Lateral semicircular canal (average)	–	–	0.34	–
Rostral semicircular canal (average)	–	–	0.52	–
Caudal semicircular canal (average)	–	–	0.55	–

but also CCMGE 628/12457 (*Sues et al., 2015*: fig. 3B, C, E; *Witmer, 2019*) and *S. musacchioi* (*Martínez et al., 2016*: figs 9C, S1), for instance, which are certainly more basal, the abducens nerve and the pituitary are farther apart than in FAM 03.064. Likewise, we do not place too much systematic importance either on the observed variations of angles between the planes of ipsilateral semicircular canals. First and foremost, these characters are deeply dependent on the degree of deformation of the specimens. We must also recall that the relative developments of the vestibular system are distinctly different from one another in braincases referred to *G. brancai* (*Knoll et al., 2014*), suggesting weak stabilizing selection on the vestibular labyrinth (which, in turn, might be related to relatively sluggish behaviour and/or little reliance on highly coordinated eye movements) in this and maybe many other sauropod species. This notwithstanding, sauropod braincases are not subject to the same selective pressures as the rest of the skeleton and as such palaeoneurology is doubtless a source of helpful further data for phylogenetic inferences (*Balanoff, Bever & Ikejiri, 2010*; *Knoll et al., 2012*; *Bronzati, Benson & Rauhut, 2018*).

A single bilateral hypoglossal canal was identified in the osteological description of FAM 03.064 (*Díez Díaz et al., 2012*). The CT data reveals that this was the caudal component of a pair of rami, the rostral constituent of which is very close to the metotic group (left side) or not clearly individualised from it (right side). A single hypoglossal root (XII) was considered characteristic of titanosaurs (*Paulina Carabajal, 2012*), but it rapidly turned out that several members of the group show two roots (see e.g., *Sues et al., 2015*; *Martínez et al., 2016*). As two hypoglossal roots are seen in the basal titanosauriforms *G. brancai* (*Knoll & Schwarz-Wings, 2009*), *E. holgeri* (*Schmitt, Knoll & Tschopp, 2015*) and indeed most sauropods, this represents the plesiomorphic condition. This character-state suggests that the titanosaur from Fox-Amphoux-Métisson is more primitive than the roughly coeval Lo Hueco lithostrotians and the distinctly more recent *J. septentrionalis* as well as, in fact, all the titanosaurs with a single hypoglossal rootlet on the endocast, such as *B. reigi* (*Paulina Carabajal, 2012*: figs 2A, 3), the derived non-saltasaurid *Diamantinasaurus matildae* (*Poropat et al., 2016*: fig. 5c, d) and the basalmost lithostrotian (clade specifier) *M. dixeyi* (*Andrzejewski et al., 2019*: figs 2A, C, S1). We suspect that the rostral hypoglossal canal coalesced with the cavum metoticum in a derived clade of titanosaurs resulting in an apparent single hypoglossal branch in the neurocranial endocasts of the taxa belonging to this lineage. Data are too deficient to trace a definite

pattern across the phylogeny of titanosaurs. Nevertheless, the rostral hypoglossal canal is fairly equidistant from that shared by the glossopharyngeal and vagoaccessory nerves rostrally and the one for the caudal hypoglossal root caudally in *S. musacchioi* (Martínez et al., 2016: figs 9C, S1), whereas it is noticeably closer to the metotic group in a more derived form like the Dzharakuduk sauropod (Sues et al., 2015: fig. 3C; Witmer, 2019). Furthermore, even though this is not an analogous phenomenon, it should be remarked that an ontogenetical trend for the most rostral embryonic hypoglossal canal to unite with the vagal canal is known in sauropsids (Starck, 1979: pp. 16-17). The fact that the rostral hypoglossal appears to have merged with the metotic group on one side but not on the other might support an intermediate position of FAM 03.064 within the phylogeny of titanosaurs between taxonomic units such as CCMGE 628/12457 (showing metotic group and rostral hypoglossal well separated on both sides; Sues et al., 2015: fig. 3A, C; Witmer, 2019) basally and others such as *L. pandafilandi* (with no visible rostral hypoglossal on either side; Knoll et al., 2013: figs 3A, D, S1, S2, S3) apically.

The phylogenetic position of the Uzbek specimen CCMGE 628/12457 is especially relevant to the present work because FAM 03.064 appears more derived in virtually every aspect. The Bissekty Formation sauropod has been recently regarded as a possible non-lithostrotian titanosaur on the basis of the absence of definitive sauropod osteoderms among the numerous vertebrate remains collected from the original site, Dzharakuduk (Averianov & Sues, 2017: p. 189). Nevertheless, bones of sauropods are extremely rare at Dzharakuduk and similar localities (Nesov, 1995: p. 20), and titanosaurian osteoderms are generally scarcely found (D'Emic, Wilson & Chatterjee, 2009), even in sites in which these sauropods are common (see e.g., Bellevue in France, Le Loeuff et al., 1994, and Lo Hueco in Spain, Vidal, Ortega & Sanz, 2014). More importantly, the possession of osteoderms is at best an ambiguous synapomorphy of Lithostrotia (see e.g., D'Emic, 2012: table 5) and, very probably, not all members of this clade bore such bony structures (see Martínez et al., 2004). Averianov & Sues (2017: p. 192) noted that the Dzharakuduk sauropod presents similarities to *Dongyangosaurus sinensis* and *Baotianmansaurus henanensis*. According to Mannion et al. (2013: p. 158), *D. sinensis*, and possibly *B. henanensis* as well, would represent a titanosaur with close relationships to *Opisthocoelicaudia skarzynskii*. However, *D. sinensis* and *B. henanensis* were later recovered as non-lithostrotian titanosaurs (Mannion, Allain & Moine, 2017: fig. 39, 2019a: fig. 5, 2019b: fig. 42), more in line with the view of Averianov & Sues (2017: pp. 192–193). If we adopt a parsimonious approach and assume that the reduction in the number of hypoglossal roots to one occurred only once at the ancestral node of Lithostrotia (or even more basally, at some point along the branch leading from the basalmost node of Titanosauria to Lithostrotia) and no reversal happened thereafter, then the titanosaur from Dzharakuduk cannot be a member of Lithostrotia, nor can *S. musacchioi*, which also show two hypoglossal rami (Martínez et al., 2016: figs 9A, C, S1). Whether or not CCMGE 628/12457 and *S. musacchioi* belong in Lithostrotia, their respective phylogenetic position with one another and with regard to the Late Cretaceous titanosaurs from Eurasia and India that have been primarily considered in the present study can be reasonably determined, with some caution due to the impossibility of assessing individual variation (Fig. 4).

The reduced inner ear labyrinth of the Dzharakuduk sauropod suggests that it is more derived than *S. musacchioi*, whereas the thickness and convolutedness of its dural membrane and the related development of the associated venous sinuses and emissary veins (see below) implies that it is less advanced than the titanosaur from Fox-Amphoux-Métisson and *a fortiori* those with a single hypoglossal branch.

The distinct narrow channel that runs from the facial foramen down to the ventral border of the parabasisphenoid of FAM 03.064 (as preserved—most of this bone is lacking; [Díez Díaz et al., 2012](#): figs 4, 5E, F) may also carry some phylogenetic information. No such groove is visible on the braincase of the Lithostrotia indet. from Lo Hueco ([Knoll et al., 2015](#)), but a similar feature is present on a fragmentary neurocranial wall recently described and attributed to *Atsinganosaurus velauciensis* ([Díez Díaz et al., 2018](#): fig. 2A). *A. velauciensis* is a titanosaur from the Campanian of Velaux-La Bastide Neuve ([García et al., 2010](#)). Velaux-La Bastide Neuve is only about 70 km from Fox-Amphoux-Métisson and the sediments of the two localities have presumably deposited in a short temporal interval around the transition from the Middle Campanian to the Late Campanian (see [Leleu, Ghienne & Manatschal, 2005](#); [Cojan & Moreau, 2006](#)). Recent phylogenetic results suggest that *Atsinganosaurus* is a more basal opisthocoelicaudiine than taxa such as *Lohuecotitan* and *Lirainosaurus* ([Sallam et al., 2018](#): fig. 3; [Gorscak & O'Connor, 2019](#): fig. 29). This may well hold true for the Fox-Amphoux-Métisson titanosaur as well.

The fact that the junction of the antotic and prootic crests constitutes the ventral border of the trigeminal foramen in FAM 03.064 makes this region of the lateral wall of the braincase similar to that in MPCM-HUE-1667 ([Knoll et al., 2015](#): figs 3C, S1) but notably different from that in *G. brancai* ([Janensch, 1935–1936](#): figs 2, 5), where these two crests converge much more ventrally. Titanosauriforms more derived than *G. brancai*, such as *M. dixeyi* ([Andrzejewski et al., 2019](#): figs 1A, B, S1) and CCMGE 628/12457 ([Sues et al., 2015](#); [Witmer, 2019](#)), also appear more primitive than FAM 03.064 in having these crests providing a space for the possible accommodation of a ventral branch of the trigeminal nerve.

As alluded to above, the level of development of the dorsal-head/caudal-middle-cerebral vein system has also a bearing on our appreciation of the phylogenetic position of FAM 03.064. This structure is particularly elaborated in *Spinophorosaurus nigerensis* ([Knoll et al., 2012](#): figs 4A, B, D, S1, S2, S3), which is likely a basal sauropod ([Holwerda & Pol, 2019](#)). Generally speaking, it is well developed in sauropods (see e.g., [Witmer et al., 2008](#)), including non-titanosaurian titanosauriforms such as *G. brancai* ([Knoll & Schwarz-Wings, 2009](#): figs 1, 2A, B, C, D) and *Tambatitanis amicitiae* ([Saegusa & Ikeda, 2014](#): fig. 4F). However, it is unnoticeable in derived titanosaurs such as those from Lo Hueco ([Knoll et al., 2013](#): figs 3A, B, C, S1, S2, S3; [Knoll et al., 2015](#): figs 4, 5B, D, S1), *J. septentrionalis* ([Wilson et al., 2009](#): fig. 7A) and possibly the other titanosaurs from India mentioned by [Witmer et al. \(2008](#): p. 76). Therefore, the degree of expansion of this complex on the endocast of the titanosaur from Fox-Amphoux-Métisson supports a position more basal within the phylogeny of Titanosauria than that of those Late Cretaceous taxa from Eurasia and India. On the other hand, the sauropod from Fox-Amphoux-Métisson appears closer to them than to the titanosaur from Uzbekistan ([Sues et al., 2015](#): fig. 3A, B, D;

Witmer, 2019) in the lack of prominent dural expansion on the dorsal surface of the hindbrain (Fig. 4).

Finally, we suggest that FAM 03.064 is not overly closely related to the only other titanosaur named from the uppermost Cretaceous of France for which neurocranial material is available, *Ampelosaurus atacis* (see Díez Díaz *et al.*, 2012: p. 635). The latter appears closer to Spanish lithostrotians such as those of the Lo Hueco site, which presumably branched further from the base of Titanosauria than the Fox-Amphoux-Métisson sauropod did (Fig. 4). Palaeoneurological investigations into *A. atacis* would provide valuable data concerning the respective phylogenetic positions—and biogeographical history—of the titanosaurs from the latest Late Cretaceous of Var, Aude and Cuenca.

CONCLUSION

The palaeoneurology of the titanosaurian braincase from the Campanian of Fox-Amphoux-Métisson reveals a number of characters of possible phylogenetic interest. These include the courses or number of canals followed by certain cranial nerves. The degree of development of the dural envelope and the associated venous channels in FAM 03.064 also appears to be indicative of its phylogenetic position within Titanosauria. Although not all the characters of FAM 03.064 may hint at a consistent phylogenetic position, the discrepancies are reasonable. This specimen appears to be from a species distinctly more advanced than the titanosaur from the lower Upper Cretaceous of Dzharakuduk (Sues *et al.*, 2015), which exhibits a developed dura, but possibly less derived than those from the upper Upper Cretaceous of Lo Hueco (Knoll *et al.*, 2013, 2015), which have only a single bilateral hypoglossal root. However, as the pattern of modification of the neurocranium within the evolution of Titanosauria is still poorly known, a number of features such as the level of thickness and morphological complexity of dural expansions in this group of sauropods might be more plastic than here considered. The growing number of studies such as this one in concert with an ever-consolidating phylogenetic framework will gradually but quite certainly enable a more positive picture of neurocranial changes during titanosaurian evolution to emerge.

INSTITUTIONAL ABBREVIATIONS

CCMGE	Chernyshev's Central Museum of Geological Exploration, Saint Petersburg, Russia
FAM	Mairie de Fox-Amphoux, Fox-Amphoux, France
GSI	Geological Survey of India, Kolkata, India
ISI	Indian Statistical Institute, Kolkata, India
MB.R.	Collection of fossil Reptilia, Museum für Naturkunde, Berlin, Germany
MDT-PV	Museo Desiderio Torres-Paleovertebrados, Sarmiento, Argentina
MPCM	Museo de Paleontología de Castilla-La Mancha, Cuenca, Spain

ACKNOWLEDGEMENTS

A. Mazurier (IC2MP, University of Poitiers) performed the scanning of the specimen. The assistance of the Association de Recherches Paléontologiques du Var (Fox-Amphoux),

particularly its president, G. Vilanova, and the Fox-Amphoux municipality is acknowledged. Constructive comments from the handling academic editor, A. Farke (Raymond M. Alf Museum of Paleontology, Claremont), and the reviewers, K. Andrzejewski (Southern Methodist University, Dallas) and M. Bronzati Filho (Universidade de São Paulo, Ribeirão Preto), improved the manuscript. X. Pereda-Suberbiola is a member of the Basque Government Research Group IT1418-19. F. Knoll is an ARAID Senior Researcher and a member of the Government of Aragon Research Group E04_17R.

ADDITIONAL INFORMATION AND DECLARATIONS

Funding

Xabier Pereda Suberbiola is supported by the research project CGL2017-85038-P (funded by FEDER/Spanish Ministry of Science, Innovation and Universities-State Research Agency). This article is a contribution to the research project CGL2017-89123-P (funded by FEDER/Spanish Ministry of Science, Innovation and Universities-State Research Agency) of which Fabien Knoll is the PI. The funders had no role in study design, data collection and analysis, decision to publish, or preparation of the manuscript.

Grant Disclosures

The following grant information was disclosed by the authors:
FEDER/Spanish Ministry of Science, Innovation and Universities-State Research Agency: CGL2017-85038-P and CGL2017-89123-P.

Competing Interests

Fabien Knoll is an Academic Editor for PeerJ.

Author Contributions

- Fabien Knoll conceived and designed the experiments, performed the experiments, analyzed the data, prepared figures and/or tables, authored or reviewed drafts of the paper, approved the final draft.
- Stephan Lautenschlager performed the experiments, analyzed the data, prepared figures and/or tables, authored or reviewed drafts of the paper, approved the final draft.
- Xavier Valentin analyzed the data, contributed reagents/materials/analysis tools, authored or reviewed drafts of the paper, approved the final draft.
- Verónica Díez Díaz analyzed the data, authored or reviewed drafts of the paper, approved the final draft.
- Xabier Pereda Suberbiola analyzed the data, authored or reviewed drafts of the paper, approved the final draft.
- Géraldine Garcia analyzed the data, contributed reagents/materials/analysis tools, authored or reviewed drafts of the paper, approved the final draft.

Data Availability

The following information was supplied regarding data availability:

The CT scan data and Avizo label files are available at: https://www.morphosource.org/Detail/ProjectDetail/Show/project_id/851.

Supplemental Information

Supplemental information for this article can be found online at <http://dx.doi.org/10.7717/peerj.7991#supplemental-information>.

REFERENCES

- Andrzejewski KA, Polcyn MJ, Winkler DA, Gomani Chindebvu E, Jacobs LL. 2019.** The braincase of *Malawisaurus dixeyi* (Sauropoda: Titanosauria): a 3D reconstruction of the brain endocast and inner ear. *PLOS ONE* **14**(2):e0211423 DOI [10.1371/journal.pone.0211423](https://doi.org/10.1371/journal.pone.0211423).
- Averianov A, Sues H-D. 2017.** Review of Cretaceous sauropod dinosaurs from Central Asia. *Cretaceous Research* **69**:184–197 DOI [10.1016/j.cretres.2016.09.006](https://doi.org/10.1016/j.cretres.2016.09.006).
- Balanoff AM, Bever GS, Ikejiri T. 2010.** The braincase of *Apatosaurus* (Dinosauria, Sauropoda) based on computed tomography of a new specimen, with comments on variation and evolution in sauropod neuroanatomy. *American Museum Novitates* **3677**:1–29 DOI [10.1206/591.1](https://doi.org/10.1206/591.1).
- Benson RBJ, Campione NE, Carrano MT, Mannion PD, Sullivan C, Upchurch P, Evans DC. 2014.** Rates of dinosaur body mass evolution indicate 170 million years of sustained ecological innovation on the avian stem lineage. *PLOS Biology* **12**(5):e1001853 DOI [10.1371/journal.pbio.1001853](https://doi.org/10.1371/journal.pbio.1001853).
- Bonaparte JE, Coria R. 1993.** Un nuevo y gigantesco saurópodo titanosaurio de la Formación Rio Limay (Albiano-Cenomanio) del la Provincia del Neuquén, Argentina. *Ameghiniana* **30**:271–282.
- Bronzati M, Benson RBJ, Rauhut OWM. 2018.** Rapid transformation in the braincase of sauropod dinosaurs: integrated evolution of the braincase and neck in early sauropods? *Palaeontology* **61**(2):289–302 DOI [10.1111/pala.12344](https://doi.org/10.1111/pala.12344).
- Bronzati M, Rauhut OWM, Bittencourt JS, Langer MC. 2017.** Endocast of the Late Triassic (Carnian) dinosaur *Saturnalia tupiniquim*: implications for the evolution of brain tissue in Sauropodomorpha. *Scientific Reports* **7**(1):11931 DOI [10.1038/s41598-017-11737-5](https://doi.org/10.1038/s41598-017-11737-5).
- Calvo JO, Gonzalez Riga B. 2019.** *Baalsaurus mansillai* gen. et sp. nov. a new titanosaurian sauropod (Late Cretaceous) from Neuquén, Patagonia, Argentina. *Anais da Academia Brasileira de Ciências* **91**(suppl 2):e20180661 DOI [10.1590/0001-3765201820180661](https://doi.org/10.1590/0001-3765201820180661).
- Cojan I, Moreau M-G. 2006.** Correlation of terrestrial climatic fluctuations with global signals during the Upper Cretaceous-Danian in a compressive setting (Provence, France). *Journal of Sedimentary Research* **76**(3):589–604 DOI [10.2110/jsr.2006.045](https://doi.org/10.2110/jsr.2006.045).
- Curry Rogers K, Forster CA. 2004.** The skull of *Rapetosaurus krausei* (Sauropoda: Titanosauria) from the Late Cretaceous of Madagascar. *Journal of Vertebrate Paleontology* **24**(1):121–144 DOI [10.1671/A1109-10](https://doi.org/10.1671/A1109-10).
- D’Emic MD. 2012.** The early evolution of titanosauriform sauropod dinosaurs. *Zoological Journal of the Linnean Society* **166**(3):624–671 DOI [10.1111/j.1096-3642.2012.00853.x](https://doi.org/10.1111/j.1096-3642.2012.00853.x).
- D’Emic MD, Wilson JA, Chatterjee S. 2009.** The titanosaur (Dinosauria: Sauropoda) osteoderm record: review and first definitive specimen from India. *Journal of Vertebrate Paleontology* **29**(1):165–177 DOI [10.1671/039.029.0131](https://doi.org/10.1671/039.029.0131).

- Díez Díaz V, Garcia G, Knoll F, Pereda Suberbiola X, Valentin X. 2012. New cranial remains of titanosaurian sauropod dinosaurs from the Late Cretaceous of Fox-Amphoux-Métisson (Var, SE France). *Proceedings of the Geologists' Association* **123**(4):626–637 DOI [10.1016/j.pgeola.2012.04.002](https://doi.org/10.1016/j.pgeola.2012.04.002).
- Díez Díaz V, Garcia G, Pereda-Suberbiola X, Jentgen-Ceschino B, Stein K, Godefroit P, Valentin X. 2018. The titanosaurian dinosaur *Atsinganosaurus velauciensis* (Sauropoda) from the Upper Cretaceous of southern France: new material, phylogenetic affinities, and palaeobiogeographical implications. *Cretaceous Research* **91**:429–456 DOI [10.1016/j.cretres.2018.06.015](https://doi.org/10.1016/j.cretres.2018.06.015).
- Díez Díaz V, Mocho P, Paramo A, Escaso F, Marcos-Fernandez F, Sanz JL, Ortega F. 2016. A new titanosaur (Dinosauria, Sauropoda) from the Upper Cretaceous of Lo Hueco (Cuenca, Spain). *Cretaceous Research* **68**:49–60 DOI [10.1016/j.cretres.2016.08.001](https://doi.org/10.1016/j.cretres.2016.08.001).
- Ferreira-Cardoso S, Araújo R, Martins NE, Martins GG, Walsh S, Martins RMS, Kardjilov N, Manke I, Hilger A, Castanhinha R. 2017. Floccular fossa size is not a reliable proxy of ecology and behaviour in vertebrates. *Scientific Reports* **7**(1):2005 DOI [10.1038/s41598-017-01981-0](https://doi.org/10.1038/s41598-017-01981-0).
- Garcia G, Amico S, Fournier F, Thouand E, Valentin X. 2010. A new titanosaur genus (Dinosauria, Sauropoda) from the Late Cretaceous of southern France and its paleobiogeographic implications. *Bulletin de la Société géologique de France* **181**(3):269–277 DOI [10.2113/gssgfbull.181.3.269](https://doi.org/10.2113/gssgfbull.181.3.269).
- Gorscak E, O'Connor PM. 2019. A new African titanosaurian sauropod dinosaur from the middle Cretaceous Galula Formation (Mtuka Member), Rukwa Rift Basin, southwestern Tanzania. *PLOS ONE* **14**(2):e0211412 DOI [10.1371/journal.pone.0211412](https://doi.org/10.1371/journal.pone.0211412).
- Hallett M, Wedel MJ. 2016. *The sauropod dinosaurs: life in the age of giants*. Baltimore: Johns Hopkins University Press. xv + 320 pp.
- Holwerda FM, Pol D. 2019. Phylogenetic analysis of Gondwanan basal eusauropods from the Early-Middle Jurassic of Patagonia, Argentina. *Spanish Journal of Palaeontology* **33**(2):289–298 DOI [10.7203/sjp.33.2.13604](https://doi.org/10.7203/sjp.33.2.13604).
- Huene Fv, Matley CA. 1933. The Cretaceous Saurischia and Ornithischia of the central provinces of India. *Memoirs of the Geological Survey of India* **21**:1–74.
- Janensch W. 1935–1936. Die Schädel der Sauropoden *Brachiosaurus*, *Barosaurus* und *Dicraeosaurus* aus den Tendaguruschichten Deutsch-Ostafrikas. *Palaeontographica, Supplement* **7**:145–298.
- Knoll F, Ridgely RC, Ortega F, Sanz JL, Witmer LM. 2013. Neurocranial osteology and neuroanatomy of a Late Cretaceous titanosaurian sauropod from Spain (*Ampelosaurus* sp.). *PLOS ONE* **8**(1):e54991 DOI [10.1371/journal.pone.0054991](https://doi.org/10.1371/journal.pone.0054991).
- Knoll F, Ridgely RC, Schwarz-Wings D, Witmer LM. 2014. The brain and inner ear of the sauropod dinosaurs from Tendaguru (Tanzania) in the context of sauropod evolution: a unique glimpse into the sensory world of Gondwanan Jurassic giants. *Journal of Vertebrate Paleontology* **34**:160.
- Knoll F, Schwarz-Wings D. 2009. Palaeoneuroanatomy of *Brachiosaurus*. *Annales de Paléontologie* **95**:165–175.
- Knoll F, Witmer LM, Ortega F, Ridgely RC, Schwarz-Wings D. 2012. The braincase of the basal sauropod dinosaur *Spinophorosaurus* and 3D reconstructions of the cranial endocast and inner ear. *PLOS ONE* **7**(1):e30060 DOI [10.1371/journal.pone.0030060](https://doi.org/10.1371/journal.pone.0030060).
- Knoll F, Witmer LM, Ridgely RC, Ortega F, Sanz JL. 2015. A new titanosaurian braincase from the Cretaceous “Lo Hueco” locality in Spain sheds light on neuroanatomical evolution within Titanosauria. *PLOS ONE* **10**(10):e0138233 DOI [10.1371/journal.pone.0138233](https://doi.org/10.1371/journal.pone.0138233).

- Lautenschlager S. 2014.** Palaeontology in the third dimension: a comprehensive guide for the integration of three-dimensional content in publications. *Paläontologische Zeitschrift* **88**:111–121.
- Le Loeuff J, Buffetaut E, Cavin L, Martin M, Martin V, Tong H. 1994.** An armoured titanosaurid sauropod from the Late Cretaceous of Southern France and the occurrence of osteoderms in the Titanosauridae. *Gaia* **10**:155–159.
- Leleu S, Ghienne J-F, Manatschal G. 2005.** Upper Cretaceous-Palaeocene basin-margin alluvial fans documenting interaction between tectonic and environmental processes (Provence, SE France). *Geological Society, London, Special Publications* **251(1)**:217–239 DOI [10.1144/GSL.SP.2005.251.01.15](https://doi.org/10.1144/GSL.SP.2005.251.01.15).
- Mannion PD, Allain R, Moine O. 2017.** The earliest known titanosauriform sauropod dinosaur and the evolution of Brachiosauridae. *PeerJ* **5(8)**:e3217 DOI [10.7717/peerj.3217](https://doi.org/10.7717/peerj.3217).
- Mannion PD, Upchurch P, Barnes RN, Mateus O. 2013.** Osteology of the Late Jurassic Portuguese sauropod dinosaur *Lusotitan atalaiensis* (Macronaria) and the evolutionary history of basal titanosauriforms. *Zoological Journal of the Linnean Society* **168(1)**:98–206 DOI [10.1111/zoj.12029](https://doi.org/10.1111/zoj.12029).
- Mannion PD, Upchurch P, Jin X, Zheng W. 2019a.** New information on the Cretaceous sauropod dinosaurs of Zhejiang Province, China: impact on Laurasian titanosauriform phylogeny and biogeography. *Royal Society Open Science* **6(8)**:191057 DOI [10.1098/rsos.191057](https://doi.org/10.1098/rsos.191057).
- Mannion PD, Upchurch P, Schwarz D, Wings O. 2019b.** Taxonomic affinities of the putative titanosaurs from the Late Jurassic Tendaguru Formation of Tanzania: phylogenetic and biogeographic implications for eusauropod dinosaur evolution. *Zoological Journal of the Linnean Society* **185(3)**:784–909 DOI [10.1093/zoolinnean/zly068](https://doi.org/10.1093/zoolinnean/zly068).
- Marsh OC. 1878.** Principal characters of American Jurassic dinosaurs: Part I. *The American Journal of Science and Arts* **16(95)**:411–416 DOI [10.2475/ajs.s3-16.95.411](https://doi.org/10.2475/ajs.s3-16.95.411).
- Marsh OC. 1880.** Principal characters of American Jurassic dinosaurs: Part III. *The American Journal of Science* **19(111)**:253–259 DOI [10.2475/ajs.s3-19.111.253](https://doi.org/10.2475/ajs.s3-19.111.253).
- Martínez RD, Giménez O, Rodríguez J, Luna M, Lamanna MC. 2004.** An articulated specimen of the basal titanosaurian (Dinosauria: Sauropoda) *Epachthosaurus sciuttoi* from the early Late Cretaceous Bajo Barreal Formation of Chubut Province, Argentina. *Journal of Vertebrate Paleontology* **24(1)**:107–120 DOI [10.1671/9.1](https://doi.org/10.1671/9.1).
- Martínez RDF, Lamanna MC, Novas FE, Ridgely RC, Casal GA, Martínez JE, Vita JR, Witmer LM. 2016.** A basal lithostrotian titanosaur (Dinosauria: Sauropoda) with a complete skull: implications for the evolution and paleobiology of Titanosauria. *PLOS ONE* **11(4)**:e0151661 DOI [10.1371/journal.pone.0151661](https://doi.org/10.1371/journal.pone.0151661).
- Nesov LA. 1995.** *Dinosaurs of northern Eurasia: new data about assemblages, ecology and paleobiogeography*. Saint Petersburg: Saint Petersburg State University, 156 pp. + 14 pls. [In Russian].
- Owen R. 1842.** Report on British fossil reptiles. *Report of the British Association for the Advancement of Science* **11**:60–294.
- Paulina Carabajal A. 2012.** Neuroanatomy of titanosaurid dinosaurs from the Upper Cretaceous of Patagonia, with comments on endocranial variability within Sauropoda. *Anatomical Record* **295(12)**:2141–2156 DOI [10.1002/ar.22572](https://doi.org/10.1002/ar.22572).
- Paulina Carabajal A, Canale JI, Haluza A. 2016.** New rebbachisaurid cranial remains (Sauropoda, Diplodocoidea) from the Cretaceous of Patagonia, Argentina, and the first endocranial description for a South American representative of the clade. *Journal of Vertebrate Paleontology* **36(5)**:e1167067 DOI [10.1080/02724634.2016.1167067](https://doi.org/10.1080/02724634.2016.1167067).

- Paulina Carabajal A, Carballido JL, Currie PJ. 2014.** Braincase, neuroanatomy and neck posture of *Amargasaurus cazaui* (Sauropoda: Dicraeosauridae) and its implications for understanding head posture in sauropods. *Journal of Vertebrate Paleontology* 34(4):870–882 DOI 10.1080/02724634.2014.838174.
- Paulina Carabajal A, Coria RA, Chiappe LM. 2008.** An incomplete Upper Cretaceous titanosaur (Sauropoda) braincase: new insights on the dinosaurian inner ear and endocranium. *Cretaceous Research* 29(4):643–648 DOI 10.1016/j.cretres.2008.01.011.
- Paulina Carabajal A, Coria RA, Currie PJ, Koppelhus EB. 2018.** A natural cranial endocast with possible dicraeosaurid (Sauropoda, Diplodocoidea) affinities from the Lower Cretaceous of Patagonia. *Cretaceous Research* 84:437–441 DOI 10.1016/j.cretres.2017.12.001.
- Paulina Carabajal A, Filippi L, Knoll F. 2015.** Estudios preliminares de la neuroanatomía del titanosaurio *Narambuenatitan*, del Cretácico Superior de Patagonia. In: Brandoni D, Diederle JM, Favotti E, Fernández Osuna MA, Ferrero B, Góis F, Gottardi G, Noriega JJ, Schmidt G, Vallone E, Vezzosi RI, eds. *XXIX Jornadas argentinas de paleontología de vertebrados: libro de resúmenes*. Diamante: CICYTTP-CONICET, 65, 83 pp.
- Poropat SF, Mannion PD, Upchurch P, Hocknull SA, Kear BP, Kundrát M, Tischler TR, Sloan T, Sinapius GHK, Elliott JA, Elliott DA. 2016.** New Australian sauropods shed light on Cretaceous dinosaur palaeobiogeography. *Scientific Reports* 6(1):34467 DOI 10.1038/srep34467.
- Saegusa H, Ikeda T. 2014.** A new titanosauriform sauropod (Dinosauria: Saurischia) from the Lower Cretaceous of Hyogo. *Japan Zootaxa* 3848(1):1–66 DOI 10.11646/zootaxa.3848.1.1.
- Sallam HM, Gorscak E, O'Connor PM, El-Dawoudi IA, El-Sayed S, Saber S, Kora MA, Sertich JJW, Seiffert ER, Lamanna MC. 2018.** New Egyptian sauropod reveals Late Cretaceous dinosaur dispersal between Europe and Africa. *Nature Ecology & Evolution* 2(3):445–451 DOI 10.1038/s41559-017-0455-5.
- Sander PM, Christian A, Clauss M, Fechner R, Gee CT, Griebeler E-M, Gunga H-C, Hummel J, Mallison H, Perry SF, Preuschoft H, Rauhut OWM, Remes K, Tütken T, Wings O, Witzel U. 2011.** Biology of the sauropod dinosaurs: the evolution of gigantism. *Biological Reviews* 86(1):117–155 DOI 10.1111/j.1469-185X.2010.00137.x.
- Schmitt A, Knoll F, Tschopp E. 2015.** Paleoneurology of *Europasaurus holgeri*, an insular dwarf sauropod from northern Germany. *Journal of Vertebrate Paleontology* 35:209.
- Seeley HG. 1888.** On the classification of the fossil animals commonly named Dinosauria. *Proceedings of the Royal Society of London* 43(260):165–171 DOI 10.1098/rspl.1887.0117.
- Sereno PC, Wilson JA, Witmer LM, Whitlock JA, Maga A, Ide O, Rowe TA. 2007.** Structural extremes in a Cretaceous dinosaur. *PLOS ONE* 2(11):e1230 DOI 10.1371/journal.pone.0001230.
- Starck D. 1979.** Cranio-cerebral relations in recent reptiles. In: Gans C, Northcutt RG, Ulinsky P, eds. *Biology of the Reptilia*. Vol. 9A. London: Academic Press, 1–38, xv + 462 pp.
- Sues H-D, Averianov A, Ridgely RC, Witmer LM. 2015.** Titanosauria (Dinosauria, Sauropoda) from the Upper Cretaceous (Turonian) Bissekty Formation of Uzbekistan. *Journal of Vertebrate Paleontology* 35(1):e889145 DOI 10.1080/02724634.2014.889145.
- Vidal D, Ortega F, Sanz JL. 2014.** Titanosaur osteoderms from the Upper Cretaceous of Lo Hueco (Spain) and their implications on the armor of Laurasian titanosaurs. *PLOS ONE* 9(8):e102488 DOI 10.1371/journal.pone.0102488.
- Wilson JA. 2005.** Redescription of the Mongolian sauropod *Nemegtosaurus mongoliensis* Nowinski (Dinosauria: Saurischia) and comments on Late Cretaceous sauropod diversity. *Journal of Systematic Palaeontology* 3(3):283–318 DOI 10.1017/S1477201905001628.

- Wilson JA, D’Emic MD, Curry Rogers KA, Mohabey DM, Sen S. 2009.** Reassessment of the sauropod dinosaur *Jainosaurus* (= “*Antarctosaurus*”) *septentrionalis* from the Upper Cretaceous of India. *Contributions from the Museum of Paleontology, University of Michigan* **32**:17–40.
- Wilson JA, Pol D, Carvalho AB, Zaher H. 2016.** The skull of the titanosaur *Tapuiasaurus macedoi* (Dinosauria: Sauropoda), a basal titanosaur from the Lower Cretaceous of Brazil. *Zoological Journal of the Linnean Society* **178**(3):611–662 DOI [10.1111/zoj.12420](https://doi.org/10.1111/zoj.12420).
- Witmer LM. 2019.** Project: Titanosaur (Dinosauria, Sauropoda) braincase and brain endocast from the Upper Cretaceous of Uzbekistan. *MorphoSource.org* M43714-79648 DOI [10.17602/M2/M79648](https://doi.org/10.17602/M2/M79648).
- Witmer LM, Ridgely RC, Dufeau DL, Semones MC. 2008.** Using CT to peer into the past: 3D visualization of the brain and ear regions of birds, crocodiles, and nonavian dinosaurs. In: Endo H, Frey R, eds. *Anatomical imaging: towards a new morphology*. Tokyo: Springer, 67–88, vii + 105 pp.